Stochastic resonance in atomic optical bistability

Amitabh Joshi* and Min Xiao†
Department of Physics, University of Arkansas, Fayetteville, Arkansas 72701, USA
(Received 14 December 2005; revised manuscript received 1 March 2006; published 28 July 2006)

Stochastic resonance (SR) is experimentally demonstrated in an atomic optical bistable system consisting of three-level atoms in Λ-type configuration confined in an optical ring cavity. The optical bistable system with enhanced Kerr nonlinearity due to atomic coherence is driven by a periodic signal and a Gaussian white noise source with variable amplitude, and displays an improved output signal-to-noise ratio, a characteristic signature of SR. The measured results match qualitatively with the theoretical predictions of the generic model for the SR phenomenon.

DOI: 10.1103/PhysRevA.74.013817 PACS number(s): 42.65.Pc, 02.50.Ey, 42.50.Gy, 05.40.−a

Stochastic resonance (SR) is a quite general phenomenon appearing in climatic cycles, electronic and magnetic systems, optical systems, and biological and neuronal systems [1,2]. The essence of such interesting SR phenomena in various systems is its seemingly counterintuitive nature, i.e., adding a certain amount of noise to the input of a system can actually increase the output signal-to-noise ratio (SNR) for a signal passing through the nonlinear medium and the optimal improvement occurs at a certain noise strength. Such behavior reveals the basic nature of SR, i.e., noise can induce a resonance like effect in multistate nonlinear systems. In the past two decades, such SR effects were observed in many systems, including a simple electronic circuit, the Schmidt trigger [3], the semiconductor diode laser [4], the bidirectional ring dye laser [5], thermally induced optical bistability in semiconductors [6], and neurophysiological systems [7,8].

The generic model describing the SR phenomenon is given by [1]

$$\dot{x}(t) = -V'(x) + A_0\cos(\Omega t + \phi) + \zeta(t), \tag{1}$$

where $V(x)$ is the reflection-symmetric potential

$$V(x) = -\frac{a}{2}x^2 + \frac{b}{4}x^4. \tag{2}$$

In Eq. (1), A_0 represents the signal amplitude, Ω is the signal frequency, and ϕ is a simple phase factor. $\zeta(t)$ denotes a zero-mean Gaussian white noise with correlation function $\langle\zeta(t)\zeta(0)\rangle = 2D\delta(t)$, where D characterizes the noise amplitude. For an appropriately chosen set of parameters of a and b, the system has a double-well structure describing a standard two-state system. Equation (1) without the noise term is an overdamped, driven anharmonic oscillator with third-order nonlinearity. When a periodic signal is added to the system together with a source of noise, the SNR of the output shows a maximum at a certain noise strength D. This resonance like feature in the SNR as a function of D gives the signature of the SR phenomenon [1,2]. Under specific conditions, the output SNR can exceed the input SNR, which can be very useful in certain applications.

The system with two-level atoms inside an optical resonator can be modeled very well with a double-well potential in certain parametric regions having the well-known atomic optical bistability (AOB) [9]. Although SR behavior has been expected and theoretically studied in simple AOB systems [10], the effect has not been, to the best of our knowledge, observed experimentally in such ideal passive two-state systems. One of the main reasons for it could be the lack of controllability in the potential barrier (width and height) of the double-well potential in two-level AOB systems. In this paper, we present our experimental studies of SR in an atomic bistable system with three-level Λ-type atoms (which exhibit electromagnetically induced transparency) inside an optical ring cavity [11]. Due to the atomic coherence induced by the laser beams in the three-level atomic system, the Kerr nonlinearity of the atomic medium is greatly enhanced [12], which helps to boost the SR effect in this system at lower optical powers. Also, with an additional coupling laser beam, the bistable curve (therefore the potential barrier of the double well) can easily be controlled [11] and optimized for observing such interesting SR phenomena in this AOB system. Both the modulated signal and broadband noise are added onto the cavity input field. To avoid the issue of mechanical stability of the system, we choose to work with a periodic sinusoidal signal of moderate amplitude which has also been well discussed for SR in the literature [13,14].

The experimental setup is outlined in Fig. 1. The energy levels of the D_1 line of ^{87}Rb atoms are employed to form the required three-level system in Λ-type configuration [11] (Fig. 1 bubble). The optical ring cavity consists of three mirrors, two of which (M_1 and M_2) have about 1% and 3% transmissivities, respectively, while the third one (M_3) is almost a perfect reflector and is mounted on a piezoelectric transducer (PZT) in order to tune the cavity length. To provide magnetic shielding, the rubidium vapor cell is wrapped in μ-metal foil and then with a heating tape for controlling the atomic density. The probe laser beam [driving the transition $5S_{1/2}(F=1)\rightarrow 5P_{1/2}(F'=2)$] circulates inside the ring cavity as the cavity field while the coupling beam [driving the transition $5S_{1/2}(F=2)\rightarrow 5P_{1/2}(F'=2)$] is misaligned from the cavity axis slightly (by about a 2° angle) so it does not circulate in the cavity. The coupling and probe lasers are both extended-cavity diode lasers, frequency locked to their respective reference cavities [15]. To set and monitor the frequency detunings of the laser beams from their respective atomic transitions a saturated atomic spectroscopy setup is

*Email address: ajoshi@uark.edu
†Email: address: mxiao@uark.edu

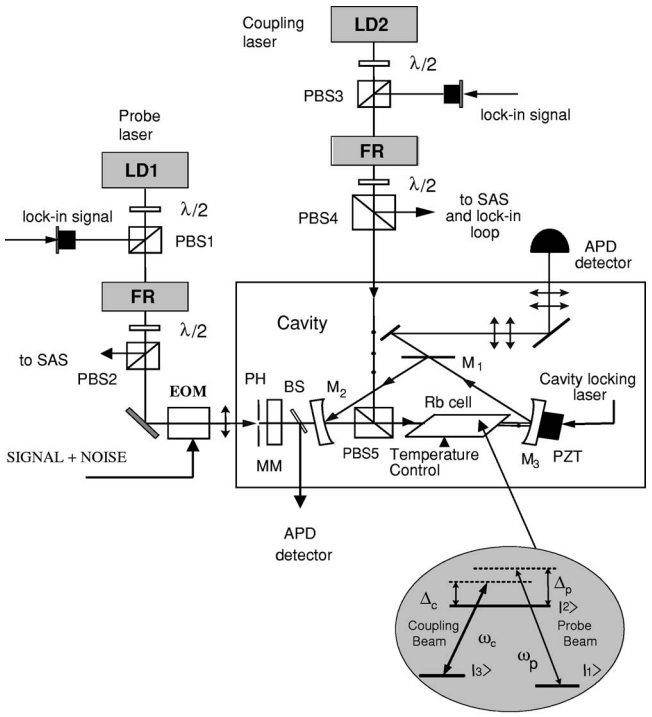

FIG. 1. Experimental setup. LD1 and LD2, diode lasers; EOM, electro-optic modulator; PBS1–PBS5, polarizing cubic beam splitters; M_1-M_3, cavity mirrors; APD, avalanche photodiode detectors; PZT, piezoelectric transducer; MM, mode-matching lens; PH, pinhole; BS, beam splitter. The bubble shows a three-level system in Λ configuration.

employed. An electro-optic modulator is introduced in the path of the probe laser before it enters the cavity (as cavity input field) to provide periodic modulation, as well as external noise from a random noise generator. By propagating the coupling and the probe (cavity) laser beams collinearly through the vapor cell containing the three-level Λ-type rubidium atoms, the first-order Doppler effect is eliminated [11].

In the experiment, several parameters can be used to control the bistable behaviors of the three-level AOB system, including the intensities and frequency detunings of the coupling laser beam and the probe laser beam, the Rb cell temperature, and the cavity frequency detuning Δ_θ. We first adjust these experimental parameters until the cavity output profile shows hysteresis loop with scanning cavity length; we then fix all parameters, turn off the cavity scanning, and lock the optical ring cavity with the help of a third diode laser [11]. To see the bistable curve in the input-output cavity field intensity plot, the electro-optic modulator is then switched on with a sawtooth signal. After establishing the proper optical bistability (here it is a refractive AOB hysteresis curve), which is monitored on the oscilloscope, the electro-optic modulator scanning is then switched off. For a refractive (two-level) AOB hysteresis curve, the parameters a and b in Eq. (2) are mainly related to the difference between the cavity resonance frequency and the optical frequency of the probe laser field, and the third-order nonlinear susceptibility of the medium, respectively [16]. However, for the three-level atomic system under consideration, both a and b are

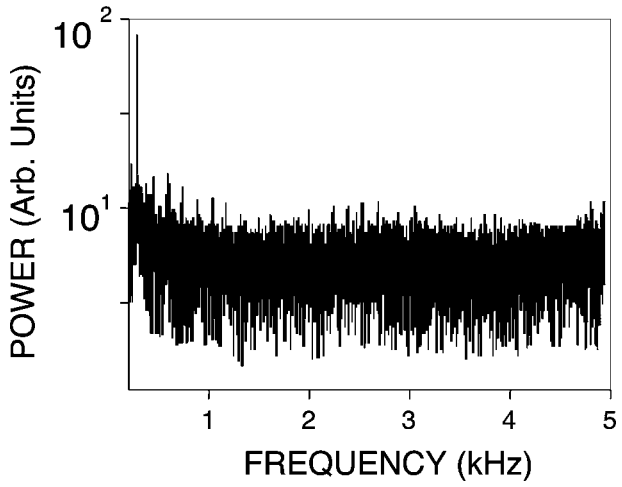

FIG. 2. A typical power spectrum (with signal frequency 150 Hz) of the output of the optical cavity with respect to the frequency.

also closely related to other experimental parameters, i.e., the probe laser frequency detuning Δ_P, the coupling laser frequency detuning Δ_C, and the coupling power P_C, etc. [17]. The cavity input power is then set in such a way that it lies in the middle of the observed AOB hysteresis curve. At this stage a sinusoidal voltage signal at 150 Hz is applied to the electro-optic modulator along with a noise voltage (the Gaussian broadband noise) generated in an arbitrary waveform generator, riding on the operating level of the cavity input laser (at the middle of the AOB hysteresis curve). A part of the electro-optic modulator output is used for monitoring the input power going into the optical ring cavity. The input as well as output optical signals of the cavity are detected with avalanche photodiode detectors. Each of the input and output waveforms as a time series is stored digitally and then a fast Fourier transform is performed on the digitized data to obtain the power spectrum. In order to obtain the averaged power spectrum the above process is repeated several times and then accumulated for averaging. A typical power spectrum of the output cavity field is shown in Fig. 2. The SNR in SR studies is defined by the ratio of the magnitudes of the power spectrum at the signal frequency, and the noise level without the input signal. This is the classical narrowband definition for SNR [1] used here. The other definition of SNR is wideband SNR, which is the ratio of the total power of the deterministic part of the signal and its harmonics in the power spectrum to the total power of the noise part [14]. The bandwidth of noise in the current experiment is limited by the response of the electro-optic modulator.

In Fig. 3(a), the experimental results of the output SNR as a function of the noise-amplitude are displayed for this system. The y axis is the SNR in linear scale while the x axis is the normalized noise amplitude, which is twice the standard deviation of the noise amplitude divided by the width of the bistable region. The choice of x axis is due to the fact that in SR, the maximum of the SNR is normally found to occur at noise variance approximately half the barrier height of the double-well potential (or at half the width of AOB hysteresis cycle in our case). Since the AOB hysteresis cycle can be

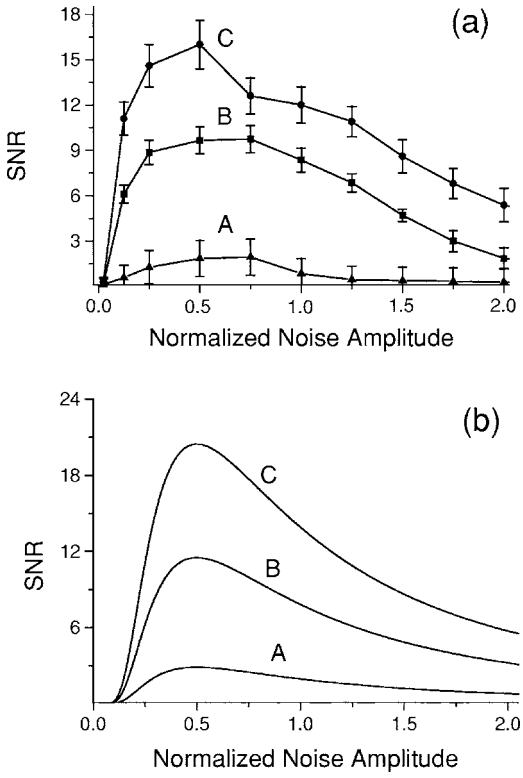

FIG. 3. (a) Experimentally measured output SNR as a function of input noise amplitude. The frequency of the sinusoidal signal is 150 Hz. Here, curves *A*, *B*, and *C* are for three different values of signal amplitudes corresponding to 10, 30, and 45 μW laser power variation about the point of operation of cavity input laser, respectively. The *x* axis represents twice the standard deviation of the noise amplitude divided by the width of the bistable region. (b) The theoretical predictions from the generic model of SR.

controlled in our experimental system very effectively and we have observed the SR phenomenon for several different OB curves, so we have normalized the noise amplitude on the *x* axis. The other experimental conditions are $T=68$ °C, $P_C=12$ mW, $\Delta_C=150$ MHz, $\Delta_P=100$ MHz, and cavity detuning $\Delta_\theta=50$ MHz. Curves *A*, *B*, and *C* are for three different values of signal amplitudes as described in the caption. For all three curves one can see that the SNR first increases with increasing noise amplitude, reaches a maximum, and then decreases down as the noise amplitude further increases. These findings were further confirmed under different experimental conditions for observing AOB. The generic model of SR describing the motion of a particle in a double-well potential [Eq. (1)] provides the basic underlying mechanism for this phenomenon in a very simplified manner [1,2]. The phenomenon of AOB can be described by a Fokker-Plank equation corresponding to the overdamped motion of a particle in a double-well potential. The upper and lower branches of the AOB hysteresis curve correspond to the two wells of the double-well potential. When the periodic signal is applied to the cavity input field, the depths of these two wells are altered periodically and the external noise works in cooperation with the signal to transfer the system from one well to another well. When noise is small, hopping between wells is rare. The hopping events increase with increasing noise strength and the SNR becomes maximum when the noise amplitude reaches an optimal value for a given signal amplitude. At very large values of noise the hopping rate is so large that the signal is lost in the background noise. This explanation is well supported by the model of Eq. (1). The problem of SR can be solved by numerical simulation of Eq. (1) for any arbitrary parametric conditions [14]. However, the phenomenon of SR is robust with respect to many physical details, e.g., the exact form and symmetry of the potential in Eq. (1) [5,13,14], so its main features can be qualitatively understood by simple considerations. In the system of AOB where fields vary adiabatically, the rate equation approach is good enough to physically model the system [1] with hopping between two minima x_+ and x_- of the double well. The periodic signal causes the well depths to change asymmetrically and noise induces transition once in a while (i.e., randomly) from one minimum to another. This process can be mathematically described by the rate equations for probabilities p_+ and p_- of finding the system around x_+ and x_- as [1,2,18]

$$\dot{p}_+(t) = -T^+ p_+ + T^- p_-,$$

$$\dot{p}_-(t) = -T^- p_- + T^+ p_+. \tag{3}$$

The hopping rate T^+ (T^-) from x_+ to x_- (x_- to x_+) follows the familiar Kramers equation $\sim\exp(-2U^{u,d}/D)$, in which $U^{u,d}=U^0[1\pm a_0\cos(\Omega t)]$ defines the time-dependent potential barrier, U^0 is the barrier height without modulation, a_0 is a quantity related to the signal amplitude, and D is the noise variance. The rate equations (3) can be solved readily to obtain the autocorrelation function and power spectrum, which give the SNR ($\mathcal{R}$) in this case to be [1,2,18]

$$\mathcal{R} = (K^2/D^2)\exp(-2U^0/D). \tag{4}$$

The parameter K is related to the signal intensity, the potential barrier, and its width. So K can be roughly calculated using the expressions for barrier height $=a^2/4b$ and barrier width $=2\sqrt{(a/b)}$ [1,2]. The parameters a and b [defined in Eq. (2)] can be approximately determined from the experimentally observed OB hysteresis curve. The numerical results for this SNR for different signals are depicted in Fig. 3(b) and are qualitatively in good agreement (curves *A*, *B*, and *C* are for the estimated parameters) with the experimental results for similar parameters as depicted in Fig. 3(a).

In order to check the dependence of the SNR on the signal frequency we have carried out measurements of the output SNR for fixed amplitudes of the noise and signal going into the optical ring cavity while changing the signal frequency from 0.15 to 2.0 kHz. The other experimental conditions are $T=74$ °C, $P_C=12$ mW, $\Delta_C=100$ MHz, $\Delta_P=40$ MHz, $\Delta_\theta=50$ MHz. From Fig. 4 (where curves *A* and *B* are for two different signal amplitudes as mentioned in the caption), it is clear that there is a small decreasing trend (within the experimental uncertainties) in the output SNR as the signal frequency increases. This observation is also in conformation with the prediction of the generic model for SR [Eq. (1)], i.e., for fixed noise and signal amplitudes there is a slight decrease in output SNR with increasing signal frequency as

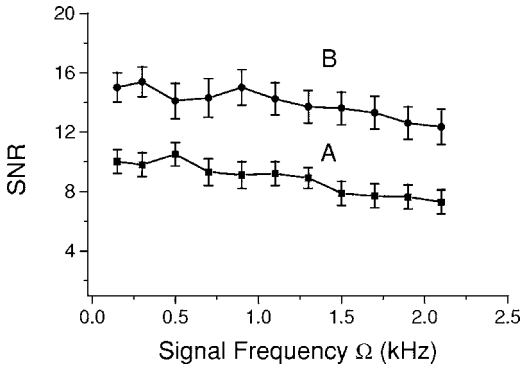

FIG. 4. Experimentally measured output SNR as a function of signal frequency for fixed normalized noise amplitude and signal amplitude. Curves *A* and *B* are for two different signal amplitudes corresponding to 30 and 50 μW laser power variation about the point of operation of the cavity input laser, respectively.

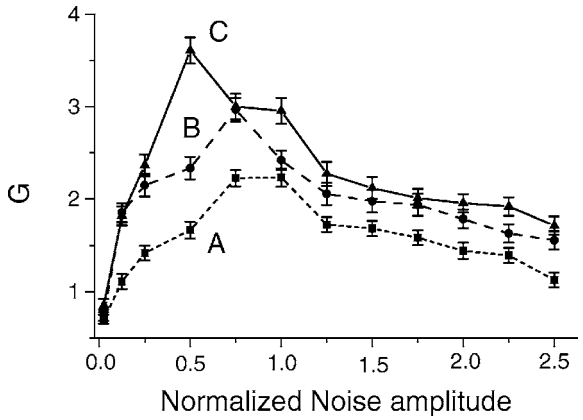

FIG. 5. Experimentally measured SNR gain *G* as a function of input noise amplitude. The curves *A* (dotted), *B* (dashed), and *C* (solid) are for the three signal amplitudes in Fig. 3(a).

Ω falls out of the range of the adiabaticity condition [1]. The adiabatic approximation for our system should be valid when $\Omega \ll a$ where a is defined in Eq. (1). This comes from the applicability of Kramers' rate formula which is derived under the assumption that the probability density within a well is roughly at equilibrium. So, for properly realizing the modified Kramers rate the signal frequency should be lower than the rate for probability to equilibrate within a well. Experimentally if the dispersive OB conditions are satisfied then this adiabaticity condition is satisfactorily achieved for low values of Ω.

To further explore the nonlinear response of the SR phenomenon in our system with enhanced nonlinearity due to atomic coherence [12] we studied the gain in SNR defined by the ratio of the output to the input SNRs, e.g., $G=(SNR)_O/(SNR)_I$. The basic definitions for input and output SNRs are the same [1,2]. In Fig. 5, G is plotted as a function of normalized noise amplitude for three different values of signal amplitude (curves *A*, *B*, and *C* are for the signal amplitudes as given in Fig. 2), with other parameters $T=74$ °C, $P_C=10$ mW, $\Delta_C=200$ MHz, $\Delta_P=30$ MHz, $\Delta_\theta=50$ MHz. The experimental parametric conditions used for these measurements are slightly different from those used in Fig. 3(a) just to demonstrate the persistence of such SR phenomenon under different physical conditions. By changing the experimental parameters in a wide range we continue to observe the SR phenomenon in this AOB system which reflects the generality and ruggedness of this interesting phenomenon for a variety of physical circumstances. The trend in the behavior of G as a function of noise amplitude is similar to what we observed for the output SNR in Fig. 3, i.e., there is a peak in the response of the system in a certain noise amplitude range. $G>1$ here in all the curves implies occurrence of a strong cooperative phenomenon such that incoherent noise power is feeding into the coherent output signal. This cooperative phenomenon could be further assisted due to the coherence generated by the electromagnetically induced transparency medium inside the optical cavity.

The passive three-level AOB system is an ideal two-state system to study this SR phenomenon since the bistable curve and therefore the shape of the double-well potential can be easily changed by the coupling beam parameters [11], which can be used to explore various properties of this interesting phenomenon. Since the linear absorption, dispersion, and Kerr nonlinearity can all be modified in such a three-level AOB system, one can carefully investigate the effects of noise transfer in this nonlinear bistable system and tunneling between the bistable states.

In summary, we studied the phenomenon of SR in a passive optical bistable system of three-level atoms in an optical cavity. This system was simultaneously driven by a periodic signal and randomized noise on top of a constant cavity input field, which led to an enhanced output SNR, confirming the nonlinear cooperative effects between signal and noise in such a system. The SR phenomenon was demonstrated under several sets of experimental parameters, which qualitatively match the predictions of the generic model. The observed large gain in SNR indicates the greatly enhanced Kerr nonlinearity in this system induced by the atomic coherence.

We acknowledge funding support from the National Science Foundation.

[1] L. Gammaitoni, P. Hanggi, P. Jung, and F. Marchesoni, Rev. Mod. Phys. **70**, 223 (1998), and references therein.
[2] T. Wellens, V. Shatokhin, and A. Buchleitner, Rep. Prog. Phys. **67**, 45 (2004), and references therein.
[3] S. Fauve and F. Heslot, Phys. Lett. **97**, 5 (1983).
[4] P. Jung and K. Wiesenfeld, Nature (London) **385**, 291 (1997).
[5] B. McNamara, K. Wiesenfeld, and R. Roy, Phys. Rev. Lett. **60**, 2626 (1988).
[6] J. Grohs *et al.*, Phys. Rev. A **49**, 2199 (1994).
[7] F. Moss and K. Wiesenfeld, Sci. Am. **273**, 50 (1995).

[8] K. Wiesenfeld and F. Moss, Nature (London) **373**, 33 (1995).
[9] See, for example, a review by L. A. Lugiato, Prog. Opt. **21**, 71 (1984), and references therein.
[10] R. Bartussek, P. Hanggi, and P. Jung, Phys. Rev. E **49**, 3930 (1994).
[11] A. Joshi, A. Brown, H. Wang, and M. Xiao, Phys. Rev. A **67**, 041801(R) (2003); A. Joshi and M. Xiao, Phys. Rev. Lett. **91**, 143904 (2003); A. Joshi, W. Yang, and M. Xiao, Phys. Rev. A **70**, 041802(R) (2004).
[12] H. Wang, D. Goorskey, and M. Xiao, Phys. Rev. Lett. **87**, 073601 (2001).
[13] M. Misono, T. Kohmoto, Y. Fukuda, and M. Kunitomo, Opt. Commun. **152**, 255 (1988).
[14] Z. Gingl, P. Makra, and R. Vajtai, Fluct. Noise Lett. **1**, L181 (2001).
[15] W. Yang, A. Joshi, H. Wang, and M. Xiao, Appl. Opt. **43**, 5547 (2004).
[16] H. Risken, C. Savage, F. Haake, and D. F. Walls, Phys. Rev. A **35**, 1729 (1987).
[17] A. Joshi, W. Yang, and M. Xiao, Opt. Lett. **38**, 905 (2005).
[18] B. McNamara and K. Wiesenfeld, Phys. Rev. A **39**, 4854 (1989).